When Van Gogh meets Mandelbrot: Multifractal Classification of Painting's Texture

Patrice Abry, Herwig Wendt, Stéphane Jaffard

When Van Gogh meets Mandelbrot: Multifractal Classification of Painting's Texture

P. Abry[(1)], H. Wendt[(2)], S. Jaffard[(3)]

[(1)] *Physics Dept., ENSLyon, CNRS, Lyon, France,*
[(2)] *Math. Dept., Purdue Univ., Lafayette, USA*
[(3)] *Math. Dept., Paris Est Univ., Créteil, France,*
patrice.abry@ens-lyon.fr, perso.ens-lyon.fr/patrice.abry

Abstract

In a recent past, there has been a growing interest for examining the potential of Image Processing tools to assist Art Investigation. Simultaneously, several research works showed the interest of using *multifractal analysis* for the description of homogeneous textures in images. In this context, the goal of the present contribution is to study the benefits of using the wavelet leader based multifractal formalism to characterize paintings. To that end, after a brief review of the key theoretical concepts, methods and tools underlying the wavelet leader based formulation of multifractal analysis, two sets of digitized painting are analyzed. The first one, the *Princeton Experiment*, consists of a set of 7 paintings and of their 7 copies, made by the same artist. It enables to examine the potential of multifractal analysis in forgery detection. The second one is composed of several partially digitized paintings by Van Gogh and contemporaries, made available by the Van Gogh and Kröller-Müller Museums (The Netherlands), in the framework of the *Image processing for Art Investigation* research program. It enables to show various differences in the regularity of the textures of Van Gogh's paintings from different periods or between Van Gogh's and contemporaries's paintings. These preliminary results plead for the constitution of interdisciplinary research teams gathering experts in art, image processing, mathematics and computer sciences.

Keywords: Image Processing, Texture Classification, Regularity, Multifractal Analysis, Wavelet Leaders, Paintings, Van Gogh, Forgery Detection, Period Dating.

Contents

1 Introduction **3**

2 Multifractal Analysis **5**
2.1 Wavelet Coefficients and Global Regularity 5
2.1.1 2D Discrete Wavelet Transform 5
2.1.2 Global regularity 6
2.2 Wavelet leader multifractal formalism 6
2.2.1 Wavelet leaders 6
2.2.2 Multifractal Formalism 7
2.3 Hölder Exponents and Multifractal Spectrum 8
2.4 Estimation Procedures 10

3 Original versus Copy: the Princeton Experiment **10**
3.1 The Princeton Experiment 10
3.2 Multifractal Properties 11
3.3 Results 12
3.3.1 Test procedure set-up 12
3.3.2 Results 13

4 Van Gogh's Paintings Multifractal Properties **15**
4.1 The Image Processing for Art Investigation research project . 15
4.2 Methodology 15
4.3 Dating Challenge 16
4.3.1 Description 16
4.3.2 Results 17
4.4 Authenticity Challenge 17
4.4.1 Description 17
4.4.2 Results 18

5 Conclusions and Perspectives **18**

6 Acknowledgements **19**

1. Introduction

Image Processing for Art Investigation. The ever growing power of digital devices (faster processors, better computers, higher resolution scanners, larger storage facilities,...) naturally and unavoidably gave birth to the desire of using such tools for Art Investigation. Yet, it is only recently, at the turn of the 3rd millennium, that conditions were met to transform this desire into some form of reality. Various research groups started to apply standard image processing tools to digitized painting, to develop new procedures or customize them to the specificities of such an application (cf. [**?**] for an example of early contribution, [**?** **?**] for review notes, and [**?**] for the presentation of state-of-the-art and joint recent research contributions). With the development of computer-assisted and statistical signal-image processing tools, the purpose of scientists is not to supplant art historians but, on the opposite, to provide them with additional material that could be extracted automatically, and using objective and reproducible criteria; this will allow progresses by diversifying the tools at hand. For paintings, it may for instance help to assess quantitative measures related to stylometry, brushstrokes, texture,... This may contribute to formulate elements of answers to questions such as deciding at which period a painting was made, detecting forgery or correctly attributing a painting to its author.

Wavelet and Fractal for Image Processing. Over the last 15 years, elaborating on multiresolution decomposition and filter banks, wavelet analysis has become one of the inescapable image processing tool. In essence, wavelet coefficients evaluate the content of an image at a given space position $\mathbf{x} = (x_1, x_2)$, and a given analysis scale a. Wavelet coefficients usually take large values when the correponding wavelet is located on any of the contours of the image while they fluctuate around small values when the wavelet is located inside smooth textures. For an introduction, review and examples, the reader is referred to e.g., [**?**]. The statistical properties of wavelet coefficients have already been successfully used in stylistic analysis of paintings and forgery detection, cf. e.g., [**?** **?** **?**].

Fractal geometry refers to an analysis paradigm that relies on the idea that the richest part of the information to be extracted from an image lies in the way the statistics of some space-scale dependent quantities vary as a function of the analysis scale a. In other words, instead of basing the analysis on the search of specific features of space-scales, it is preferred to postulate that

space-scales are all and jointly equally important and that the key information consists in the mechanisms relating ones to the others. This dependence is usually postulated in the form of power laws: a^{ζ} (with ζ referred to as the *scaling exponent*), which explains why *fractal* is also termed *scaling* or *scale invariance*. Wavelet analysis consists in decomposing an image on elementary shapes (the wavelet basis) which are all deduced from three fundamental functions, the *mother wavelets* by translation and dilation, see Eq. (1). Scaling invariance properties of the image will imply power-law behaviors of the coefficients. Therefore wavelets constitute a *natural* decomposition system for characterizing fractal properties of images. Fractal tools can be used both for the analysis of contours and textures. There is a rich literature discussing the relevance of fractal paradigms to analyze or model natural images, a recent and interesting review can be consulted in [**?**]. In the context of Art, it was used in [**?**] to characterize some of Jackson Pollock's masterpieces.

Goals, contributions and outline. Beyond *fractal* analysis, essentially aiming at characterizing how *irregular* an object is globally, typically by means of a single scaling exponent, *multifractal* analysis consists of a signal/image processing tool that concentrates on describing the fluctuations along space of the local regularity of the object, hence often requiring the potential use of a collection of scaling exponents. While popular for the analysis of 1D signal, multifractal analysis remained barely used for image processing for technical, practical and theoretical reasons (cf. a contrario [**?**]). However, this situation has recently been changed when it has been shown that a theoretically sound and practically efficient formulation of multifractal analysis could be obtained if based on wavelet leaders, a simple construction elaborating on 2D discrete wavelet transform coefficients, cf. [**?** **?** **?** **?**]. This resulted in a powerful tool for the analysis of textures in images, as detailed theoretically in [**?**] and explored practically in [**?**].

The present contribution aims at exploring the potential of the wavelet leader multifractal analysis for art painting texture classification. First (cf. Section 2), the principles and practical procedures underlying the wavelet leader multifractal analysis will be presented in a manner geared towards practitioners (hence avoiding theoretical developments and proofs, for which the reader will be referred to earlier publications). This introduction will be illustrated with results computed on various real paintings. Then (cf. Section 3), it will be shown when and how the wavelet leader multifractal analysis enables to discriminate between original paintings and copies, in the context

of an original experiment conducted by the *Machine Learning and Image Processing for Art Investigation Research Group* at Princeton University (cf. `www.math.princeton.edu/ipai/index.html`). Finally (cf. Section 4), the wavelet leader multifractal analysis will be applied to a set of Van Gogh's and contemporaries's paintings made available by the Van Gogh and Kröller-Müller Museums (The Netherlands), in the context of the *Image Processing for Art Investigation* research project (cf. `www.digitalpaintinganalysis.org/`).

2. Multifractal Analysis

2.1. Wavelet Coefficients and Global Regularity

2.1.1. 2D Discrete Wavelet Transform

An orthonormal wavelet basis in two dimensions consists in the choice of three smooth, compactly supported functions ψ^1, ψ^2, ψ^3 such that the system

$$\psi^i_{j,(k_1,k_2)}(x_1,x_2) = 2^{-j}\psi^i(2^{-j}x_1-k_1, 2^{-j}x_2-k_2), \quad j,k_1,k_2 \in \mathbb{Z}, i = 1,2,3 \quad (1)$$

constitute an orthonormal basis of $L^2(\mathbb{R}^2)$. Let $X(\mathbf{x})$ (with $\mathbf{x} = (x_1, x_2)$) denote a gray level image. We will denote by $D^m_X(j,\mathbf{k})$ (with $\mathbf{k} = (k_1, k_2)$, m $= 1, 2, 3$) the coefficients of the image X on this wavelet basis, i.e. $D^m_X(j,\mathbf{k}) = \langle X|\psi^i_{j,k}\rangle$. Note that these coefficients are not computed as integrals, but using the classical pyramidal recursive algorithm supplied by the *fast wavelet transform*. In nature, $D^m_X(j,\mathbf{k})$ measures the amount of energy of X located in the neighborhood of $(2^j k_1, 2^j k_2)$ of width $\sim 2^j$ and in the frequency bands localized around $\pm 2^{-j}$. For an introduction to the 2D Discrete Wavelet Transform (2D DWT), the reader is referred to e.g., [**?**].

In the present work, it has been chosen to work with mother wavelets obtained as tensor products of the minimal compact support Daubechies wavelet families, parametrized by their number of vanishing moments N_ψ [**?**]. It has been discussed elsewhere that this family has ideal theoretical and practical properties with respect to scaling and fractal analysis (cf. e.g., [**?**]).

The 2D DWT naturally outputs L^2 normalized wavelet coefficients, while it is now well-admitted (cf. e.g., [**?** **?**]) that for scaling or fractal analysis, a L^1 normalization, $d^{(m)}_X(j,k_1,k_2) = 2^{-j}D^{(m)}_X(j,k_1,k_2)$, is better suited and will hence be used from now on.

2.1.2. Global regularity

The wavelet coefficients $d_X^{(m)}(j, \mathbf{k})$ enable to define and measure a property of X, which plays a key role with respect to fractal analysis: Its global regularity h_m, defined as

$$h_m = \sup\{\epsilon : \ X \in C^\epsilon\}, \tag{2}$$

where $X(\mathbf{x})$ is said to belong to C^ϵ, $\epsilon \in \mathbb{R}$, iff:

$$\exists C > 0 : \quad \forall j, k_1, k_2, m \ \ |d_X^{(m)}(j, k_1, k_2)| \leq C 2^{j\epsilon}. \tag{3}$$

An intuitive interpretation of h_m is postponed to Section 2.3.

It follows from (3) that

$$h_m = \liminf_{2^j \to 0} \frac{\log\left(\sup\limits_{m,k_1,k_2} |d_X^{(m)}(j, k_1, k_2)|\right)}{\log(2^j)}. \tag{4}$$

Practically, this implies that h_m can be measured by performing linear regressions of the log of the magnitudes of the largest wavelet coefficients at scales 2^j versus the log of the scales $a = 2^j$ [**?** **?**].

2.2. Wavelet leader multifractal formalism

The purpose of multifractal analysis is to base image classification on exponents derived from power-law behaviors of space-averaged quantities computed at different scales. Several such quantities have been proposed; however, a natural interpretation of multifractal analysis (mentioned in Section 2.3) implies that a quantity more natural to consider is based on the *wavelet leaders*, which we now define.

2.2.1. Wavelet leaders

Let λ_{j,k_1,k_2} denote the dyadic square

$$\lambda_{j,k_1,k_2} = [k_1 2^j, (k_1 + 1)2^j) \times [k_2 2^j, (k_2 + 1)2^j),$$

and denote by $3\lambda_{j,k_1,k_2}$ the union of λ_{j,k_1,k_2} and its 8 closest neighbours, i.e.

$$3\lambda_{j,k_1,k_2} = [(k_1 - 1)2^j, (k_1 + 2)2^j) \times [(k_2 - 1)2^j, (k_2 + 2)2^j).$$

First, if the global regularity exponent h_m is positive, then the wavelet leaders of $L_X^{(\gamma)}$ are simply defined as [**? ? ?**]:

$$L_X^{(\gamma)}(j,k_1,k_2) = \sup_{m,\,\lambda' \subset 3\lambda_{j,k_1,k_2}} |d_X^{(m)}(\lambda')|, \tag{5}$$

The wavelet leader $L_X^{(\gamma)}(j,k_1,k_2)$ located on each node of the dyadic grid (j,k_1,k_2) is obtained by replacing the wavelet coefficient $d_X^{(m)}(j,k_1,k_2)$ by the largest of all the $|d_X^{(m)}(\lambda')|$ that are located at scales finer or equal to 2^j within a small neighborhood around the location $(x_1 = 2^j k_1, x_2 = 2^j k_2)$. This construction is illustrated in Fig. 1.

If h_m is negative, then the supremum in (5) can be infinite, in which case, one first "smoothes" the data by dividing the wavelet coefficients by a power large enough so that the supremum becomes finite. More precisely, let $\gamma \geq 0$ be defined as

$$\gamma = \begin{cases} 0 & \text{if } h_m > 0, \\ \epsilon & \text{if } h_m \leq 0. \end{cases} \tag{6}$$

where, in practice, ϵ is chosen as the multiple of $1/2$ such that $0 < \epsilon + h_m \leq 1/2$.

The wavelet leaders of $L_X^{(\gamma)}$ are defined in all cases as

$$L_X^{(\gamma)}(j,k_1,k_2) = \sup_{m,\,\lambda' \subset 3\lambda_{j,k_1,k_2}} |2^{\gamma j} d_X^{(m)}(\lambda')|. \tag{7}$$

Mathematically, this renormalization of the wavelet coefficients is equivalent to replacing the initial image by a fractional integral of order ϵ, which amounts to shift the exponent h_m of the data by ϵ.

2.2.2. Multifractal Formalism

Multifractal analysis consists in deriving power-law exponents from space averages of wavelet leaders at the scales available in the data. One can introduce an extra parameter q by actually computing space averages of the q-th order of the wavelet leaders, at a given scale $a = 2^j$: Let

$$S(2^j, q, \gamma) = \frac{1}{n_j} \sum_{k_1,k_2} L_X^{(\gamma)}(j,k_1,k_2)^q, \tag{8}$$

where n_j denotes the number of wavelet coefficients actually computed at scale $a = 2^j$. The *scaling* function of the image is then defined as

$$\zeta(q,\gamma) = \liminf_{2^j \to 0} \frac{\log(S(2^j,q,\gamma))}{\log(2^j)}. \tag{9}$$

Note that, by construction, the scaling function is concave with respect to q [**?**]. This formalism hence essentially assumes that the $S(2^j, q, \gamma)$ behave as power laws with respect to the analysis scale $a = 2^j$, in the limit of fine scales $2^j \to 0$:

$$S(2^j, q) \sim \lambda_q 2^{j\zeta(q,\gamma)} \quad \text{when} \quad j \to -\infty, \tag{10}$$

From a practical perspective, it is expected that this power law behaviors hold over a broad range of scales. Therefore, the $\zeta(q, \gamma)$ are referred to as the *scaling exponents*. These power law behaviors constitute the founding relation connecting the concepts of (multi-)fractal and scale invariance. Moreover, it is fundamental to note that Multifractal Analysis requires the use of both positive and negative values of q around 0 to fully characterize the fractal properties of X (cf. e.g., [**?** **?** **?**]), this will be further discussed in Section 2.3.

The scaling function $\zeta(q, \gamma)$ characterizes the fractal properties of the image X [**?**] and can hence be involved in any of the usual image processing tasks: Characterization, model selection, classification, detection, ... This has been successfully applied to design image classification procedure (cf. e.g., [**?**]). Scaling functions obtained from one of the *Princeton* paintings and one of the Van Gogh's paintings are illustrated in Figs. 2 and 3, bottom row.

Because the practical measure of the function $\zeta(q, \gamma)$ for all q can be tedious and its use for hypothesis testing intricate, it has been proposed to use a polynomial expansion in the neighboorhood of $q = 0$ by [**?** **?**]:

$$\zeta(q, \gamma) = \sum_{p \geq 1} c_p^{(\gamma)} \frac{q^p}{p\,!}. \tag{11}$$

Though this expansion may not be valid in certain specific cases, its power still lies in the fact that, when well-defined, the coefficients $c_p^{(\gamma)}$ can be estimated directly (without the burden of estimating the $\zeta(q, \gamma)$ themselves), as they are related to the dependence of the cumulant of order p of the quantities $\ln L_X^{(\gamma)}(j, k_1, k_2)$ (cf. [**?** **?**]). By concavity of the scaling function, note that $c_2 \leq 0$. Therefore, in practice, it is often preferred to approximate the expansion by estimating only the first values of the $c_p^{(\gamma)}$s.

2.3. Hölder Exponents and Multifractal Spectrum

The wavelet leader based multifractal formalism described in the previous section constitutes one of the most powerful tools to estimate the *multifractal*

spectrum of an image. This theoretical connection is now detailed in particular because it supplies a motivation for the use of wavelet leaders. However, the theoretical material developed in this section is not practically used for the analysis of the paintings described in the forthcoming sections.

Let $X(\mathbf{x}) : x \in \mathbb{R}^d \to X \in \mathbb{R}$ denote the function of interest, assumed to be such that its $h_m > 0$ (hence γ is set to $\gamma = 0$ for this section. For an image, $d = 2$ and $\mathbf{x} = (x_1, x_2)$.

The local regularity of X at location $\mathbf{x}_0$ can be measured by comparing $X(\mathbf{x}_0)$ to a local power law behavior: $|X(\mathbf{x}) - P_{\mathbf{x}_0}(\mathbf{x})| \leq C|\mathbf{x} - \mathbf{x}_0|^\alpha$, with $\alpha > 0$, and where $C > 0$ and P is a polynomial such that $deg(P) < \alpha$. The Hölder exponent $h(\mathbf{x}_0)$ is the largest such α.

Though theoretically based on a measure of local regularity, it is essential to point out that multifractal analysis **does not** aim at providing the user with information in the form of a space dependent function $h(\mathbf{x})$, but instead with a global measure of the spatial geometry underlying the fluctuations of h along space. This is achieved via the so-called *multifractal spectrum*, consisting of the Hausdorff dimensions $\mathcal{D}$ of the sets of locations $\mathbf{x}$, for which the Hölder exponents take the same value h: $\mathcal{D}(h) = \dim_H\{\mathbf{x} : h(\mathbf{x}) = h\}$. Because it is a dimension, the multifractal spectrum is confined to $0 \leq \mathcal{D}(h) \leq d$. By convention, $\mathcal{D}(h) = -\infty$ for the Hölder exponents that are not present in X. For theoretical introductions to multifractal analysis, the reader is referred to e.g., [**?** **?**]. Note however that, theoretically, the Hölder exponent at a point x can be recovered by a regression on la log-log scale, of the wavelet leaders located above x, with respect to the scale 2^j, see [**?**]. This explains why wavelet leaders were the natural candidates in the obtention of multifractal analysis.

It can be shown theoretically that the Legendre transform of the the scaling function $\zeta(q, 0)$ provides an upper bound of $\mathcal{D}(h)$:

$$\mathcal{D}(h) \leq \mathcal{L}(h) = \inf_{q \in \mathbb{R}} (d + qh - \zeta(q)). \tag{12}$$

For experimental data, which are never known with an infinite precision, the spectrum $\mathcal{D}(h)$ can never be computed, and, in practice $\mathcal{L}(h)$ is the only quantity that can be estimated. Therefore, with a slight abuse of language, one often calls $\mathcal{L}(h)$ the multifarctal spectrum. Also, the polynomial expansion (11) can be recast on $\mathcal{L}(h)$, starting with (cf. **??** for a complete

formula):

$$\mathcal{L}(h) \simeq d + \frac{c_2}{2}\left(\frac{h - c_1}{c_2}\right)^2, \tag{13}$$

for h close to c_1. This approximation shows that c_1 corresponds to the value of h where $\mathcal{L}(h)$ is maximal, hence to the most typical regularity exponent h observed in X, while $-c_2$ essentially measures the dispersion of the hs actually along the various locations x (explaining why this is sometimes referred to as the *strength* of the multifractality). The Legendre transform used above (cf. Eq. (12)) indicates that the obtention of the full curve $\mathcal{L}(h)$ requires the use of both positive qs (capturing the lowest hs) and negative qs (capturing the largest hs). Moreover, when positive, h_m corresponds to the smallest value of h that exists in X (i.e., for which $\mathcal{L}(h) \neq -\infty$, or in simpler words, the leftmost point of $\mathcal{L}(h)$), hence its name h_m where m stands for *minimal*.

Multifractal spectra obtained from one of the *Princeton* paintings and one of the Van Gogh's paintings are illustrated in Figs. 2, and 3 bottom row.

2.4. Estimation Procedures

The procedures to estimate practically the $\zeta(q, \gamma)$, the $c_p^{(\gamma)}$ or the function $\mathcal{L}(h)$ have been presented in detail and their performance studied in [**? ? ?**], and are hence not further recalled here. They are essentially based on weighted linear regressions in suited log-log diagrams, which are illustrated in Figs. 2 and 3, middle row, for one of the *Princeton* paintings and and one of the Van Gogh's paintings.

3. Original versus Copy: the Princeton Experiment

Appealing though it may be, applying multifractal analysis immediately and blindly to masterpieces, such as Van Gogh's paintings, to detect forgery or to classify them according to given artistic periods is difficult as in many cases conservators and art historians are often still debating on what are the correct answers and also because the direct transposition of the question must be formulated into an Image Processing language. Instead, we chose to test multifractal analysis on the *Princeton experiment* data.

3.1. The Princeton Experiment

The *Machine Learning and Image Processing for Art Investigation Research Group* at Princeton University (cf. `www.math.princeton.edu/ipai/index.html`)

had the brilliant idea of setting up a *scientific* experiment. It is described in detail at `www.math.princeton.edu/ipai/datasets.html` as well as in [**?** **?**]: Charlotte Caspers, an art conservation student from Stichting Restauratie Atelier Limburg, specializing in art reconstruction, was proposed to perform a series of seven paintings, using different materials (various brushes, canvas, paints). All of them are *small* ($\simeq 15 \times 15$ cm^2), with indoor environment still life subjects. This is described in Table 1 and the paintings shown in Fig. 4. After some delay (two weeks), she was requested to make as close as possible copies of her originals, in the same conditions, and using for each one the same materials. Original and copies were scanned at a very high resolution (800 dpi), enabling to analyze the very fine scales of the texture, (as a pixel essentially represents 32×32 μm^2). The Princeton group is gratefully acknowledged for making the material of this experiment available to other research teams.

3.2. Multifractal Properties

To analyze and assess fractal properties in paintings, small patches of $N \times N$ pixels are selected manually as pieces of homogeneous textures. Then, the wavelet leader multifractal formalism, as described in Section 2, is applied to each of them. As illustrated in Figs. 2 and 3, with $N = 1024$, the structure functions $S(j, q, \gamma)$ are satisfactorily following the power-law behavior postulated in Eq. (10), for a range of values of qs around 0, $q \in [-5 : 5]$. These hold for all 7 paintings, for both the original and the copies, for many different patches located at various places of the painting (bird, bag, upper background, lower background, ...). Other figures, in the spirit of Fig. 5, are not reported here for sake of space, but are available upon request. This hence validates that the fractal (or scaling) properties in these paintings, can be regarded as relevant features to describe their textures.

An important aspect of the wavelet leader based multifractal analysis procedure consists in the fact that the range of scales $a \in [a_m, a_{\max}]$, within which the scaling behaviors hold (as in Eq. (10)), is selected a posteriori by the expert (assisted by some statistical procedures [**?**]) from visual inspection of the log-log diagrams such as those in Fig. 2. Therefore, the selection of the relevant range of scales is not an a priori arbitrary choice but rather constitutes per se an important output of the analysis: It provides information on the scales in actual units within which fractal properties hold. For the Charlotte Casper's paintings, it can be estimated that scaling holds over a decade, with scales ranging from $[0.5 \times 0.5]$ to $[5 \times 5]$ mm^2. This

shows that scaling properties are not related to the shape or type of subject or object actually represented in the paintings, but rather to fine details of the various textures.

Furthermore, when comparing patches with the same location on the original and on the copy, it is observed that scaling properties do exist for both paintings but are different. This is illustrated in Fig. 5, where the scaling functions and the multifractal spectra significantly differ. Interestingly, it is found that the multifractal spectra estimated from the copies tend to be systematically shifted to the right on the Hölder exponent axis, compared to those measured on originals. Technically, this is effectively measured on c_1, which estimates the position of the maximum of the multifractal spectrum: It is often observed that $c_1^{(\text{copy})} > c_1^{(\text{origin.})}$. Consistently, it is observed that $h_{min}^{(\text{copy})} > h_{min}^{(\text{origin.})}$. Both these observations clearly indicate that the textures of the copies are systematically *globally more regular* and *smoother* than those of the original same patches.

3.3. Results

3.3.1. Test procedure set-up

This section aims at deciding whether the differences observed between the multifractal parameters estimated on copies and original are statistically significant, providing confirmations for or rejecting the above case observations by means of statistical procedures.

A key point in the observations described above (cf. Section 3.2) lied in the fact that multifractal analysis was applied to well-chosen patches of homogeneous textures: the bird, as in the example illustrated in Fig. 2, the bag, the backgrounds,... This requires a human/expert decision and cannot be easily automated. Here, it has been chosen instead to split each painting blindly into adjacent non-overlapping patches of $N \times N$ pixels. The wavelet leader based multifractal formalism is applied independently to each of them. The scaling range is kept fixed ($[0.5 \times 0.5]$ to $[5 \times 5]$ mm^2) according to the preliminary analysis described above. In the results reported below, patch sizes $N = 2^9, 2^{10}, 2^{11}$ have been used and yield consistent conclusions. Tables are given for $N = 2^{10}$.

Along another line, the digitized paintings are provided in the form of 3 8 bits matrices corresponding respectively to the RGB channel outputs supplied by the scanner. Systematically, these 3 channels have been transformed into a single Intensity gray-level image I, and into 3 channels corresponding

to the classical HSL (Hue, Saturation, Lightness) representation system for colors (cf. e.g., `en.wikipedia.org/wiki/HSLandHSV` for the exact definitions of the transformation RGB $\rightarrow$ I and RGB $\leftrightarrow$ HSL). For each original and copy, for each patch, these 7 instances (RGB, I, HSL) were analyzed independently.

Three characteristic multifractal parameters have been systematically retained for the test procedures: h_m, c_1 and c_2. Results shown are those obtained using the minimal compact support orthonormal Daubechies wavelet ψ with $N_\psi = 2$ vanishing moments [**?**], and are consistent with those obtained when N_ψ is increased.

To test whether significant changes are observed between the estimated multifractal parameters from original and copy, a set of classical non parametric hypothesis tests are applied and p-values are computed against the null hypothesis H_0 which holds if no change is observed. Two categories of tests where used. PairWise tests (SignTest and SignRank) compare estimates obtained from patches with same locations on original and copy. Non PairWise tests (Wilcoxon RankSum) compare globally the vectors of multifractal attributes estimated over the entire originals and copies, with no explicit reference to the locations in the painting of the estimated parameters. They are hence far more demanding, as they could be applied to sets of painting that are not copies of a set of originals. A situation which is much more likely to be of interest as it corresponds to the situation where a set of paintings that are questionably attributed to one master are tested against a set of paintings indisputably attributed to this master, but need not be copies of the reference set. The level of significance is, as classically done, set to 0.05 (i.e., differences are regarded as statistically significant whenever $p \leq 0.05$, with a 5% level of chances of incorrectly deciding so).

Tests are applied both to the multifractal parameters estimated from all 7 channels and to the L channel only (hence to a single gray-level image).

3.3.2. Results

The differences between original and copy in the estimated multifractal parameters are shown by means of box-plots in Fig. 6. The p-values resulting from the different tests are reported in Table 2. Carefully reading this table and figure yields the following observations:

- When significant, changes in c_1 and h_m are observed to occur systematically jointly and with larger values for copies compared to originals.

- Parameter c_2 is rarely found discriminant, and when so, the changes in c_2 are not systematically in the same direction.

- For Paintings 1 to 3, both PairWise and Non PairWise yields significant changes be they applied to All-Channels or to the Luminance only.

- For Paintings 5 and 7, discrimination is achieved for PairWise tests applied to All-Channels only.

- For Paintings 4 and 6, no discrimination is achieved.

Such observations induce the following humble conclusions, summarized in Table 3:

- Multifractal Properties: When significant changes are found, the multifractal spectra computed from the textures of the copies appears globally shifted to the right, with quasi no deformation: The change in h_m (the leftmost point) is comparable to the change in c_1 (location of the maximum, and c_2 (width of the spectrum) is not changed. Therefore, the textures in copies are systematically globally more regular than those of the originals, but they show neither a larger nor a smaller variability around this global regularity. Let us also recall the important fact that fractal properties are observed for scales ranging from $[0.5 \times 0.5]$ to $[5 \times 5]$ mm^2. Fractal properties may hence tentatively and for that case be related to brushstrokes, though there is no objective consensus on what scales are related to what characteristics of the paintings (cf. [**?** **?**] for interesting discussions on these issues).

- Painting Properties: Clear and obvious discriminations are achieved for the 3 first paintings whose common feature is the use of Soft & Hard brushes, while discrimination is not or barely achieved when using Soft brushes only, so that the natural conclusion is to attribute this difference to the brush actually used. The fact that the PairWise tests yield detection for paintings 5 and 7 remain to be interpreted. The reasons why no discrimination is achieved for Paintings 4 and 6 also remain to be understood. For these paintings, as shown in Fig. 7, scaling and fractal properties are equally valid as for those of other paintings but are not discriminant. In Fig. 7, a strong canvas structure is observed and may constitute the dominant feature of the texture. Because, it exists for both the original and the copy, it may prevent discrimination.

4. Van Gogh's Paintings Multifractal Properties

4.1. The Image Processing for Art Investigation research project

Let us now turn to the analysis of Van Gogh's paintings. In the framework of the *Image Processing for Art Investigation* research project (cf. `digitalpaintinganalysis.org/`) initiated by R. Johnson (Cornell University) and I. Daubechies (Princeton University), the Van Gogh and Kröller-Müller Museums (The Netherlands), made available a set of partial and low resolution digitized versions of Van Gogh's and contemporaries's paintings. For obvious reasons, high resolution copies are not completely available but *checkerboarded* on their right-half. The scanning resolution is 200dpi. To investigate the potential of image processing tools for art investigation, a series of stylometry challenges were set up under the supervision of R. Johnson, J. Coddington (MoMA, New York) and L. van Tilborgh (Van Gogh Museum, Amsterdam). These challenges are presented in details at `www.digitalpaintinganalysis.org/Challenges.htm`. In the present contribution, it has been chosen to illustrate the results obtained on the *dating* and *authenticity* challenges, described below.

4.2. Methodology

Because paintings naturally consist of different textures, they are not analyzed globally. Instead, fractal property analysis is based on the manual selection of small patches of $N \times N = 512 \times 512$ pixels for each painting. The wavelet leader multifractal formalism, described in Section 2, is applied to each of the seven channels (RGB, HSL, Intensity, cf. Section 3.3.1 above) of a patch, and the corresponding multifractal attributes $\zeta(q), D(h), h_m, c_1, c_2$ are computed.

The choice of a patch for each single painting is based on the following criteria:

- Homogeneity of texture. Patches are manually located on pieces of texture that appear homogeneous for all seven channels in order to limit the presence of large-scale coherent structures and heterogeneity potentially obstructing the analysis (such as the arms of the windmill in f503, or a combination of background and subject). Note that different channels of the same patch may reveal very different textures and structures (cf. e.g. the Red Channel of painting f452 in Fig. 9, and the Saturation Channel in Fig. 10). In addition, care has been taken to

place the patches on regions for which the painting can be assumed to have been subject to similar techniques, combinations of brushes, etc. (e.g. the heads of flowers in a bouquet, a part of the background).

- Scaling and multifractal properties. The patches are chosen based on the quality of their scaling properties, including careful inspection of the wavelet coefficient based structure functions prior to fractional integration, and theoretical constraints on parameter estimates (for instance, $c_2 \leq 0$). Furthermore, estimates for the patches are required to be stable with respect to small changes in the position of the patch.

The lower scanning resolution (compared to that in the Princeton Experiment) makes it more difficult to decide accurately on the range of scales to involve in estimation. However, scaling properties are overall found to systematically hold for all paintings in the two challenges for scales ranging from 0.5×0.5 mm^2 to 4×4 mm^2.

While some of the paintings do not leave much freedom for choosing a patch because of their limited size (e.g. f441 and s448, cf. Figs. 8 and 12, respectively), others do (e.g. f297, f392 or f411). For these, different patches could be selected for analysis. A careful inspection suggests that, within the natural statistical fluctuation of the estimation procedures, the multifractal attributes obtained on different patches from a single painting are consistent. This is illustrated in Fig. 9, where three patches for the painting f452 are compared.

4.3. Dating Challenge

4.3.1. Description

Van Gogh, while in France, had two major periods of creation, in Paris (ending early 1888) and later in Southern France (Provence). While a number a paintings of the master are unambiguously attributed to the Paris or to the Provence periods, the decision is still under debate amongst experts and art historians for a number of others. Investigations by art experts often rely on a number of material and stylometric features (density of brush strokes, size or scale of the brush strokes, thickness of contour lines, layers, colors, ...). In an attempt to investigate the potential benefits of computer-based image processing procedures to assist painting analysis, two sets of 8 paintings from the Paris and Provence period were selected as benchmark references and 3 paintings, whose dates of creation are unknown, are proposed to the

challenge. Low resolution partial and digitized copies of these three sets of Van Gogh's masterpieces are shown in Fig. 8 (nomenclature corresponds to the Van Gogh museum catalog).

4.3.2. Results

In Fig. 10, logscale diagrams, scaling functions and multifractal spectra for the Saturation Channel for an arbitrary selection of one painting for each of the three classes are illustrated. It suggests that for this example, the painting from the Provence period may show globally less regularity than the Paris period.

To attempt to further quantify this observation, we choose to analyze in more detail the reduced set c_1, c_2, h_m of point estimates obtained by the wavelet leader based multifractal analysis for all paintings. Because the recourse to machine learning (such as Support Vector Machines) for 19(= 8+8+ 3) subjects in a 42(= 7*3*2)D space does not make any sense, we instead inspected manually a large collection of 2D projections of this space. The most convincing discrimination is obtained with parameter h_m computed from the Red-Channel and c_1 from the Saturation-Channel, with the saturation channels being particularly discriminant, cf. Fig. 11. Interestingly, saturation in colors is known by art historians as one of the features used to discriminate both periods (cf. `www.digitalpaintinganalysis.org/Challenges.htm`). Note, however, that multifractal analysis does not discriminate saturation on its level but instead on the regularity of the texture in the Saturation-Channel. This projection supports the above observation that textures in Van Gogh's during the Paris period appear to be more regular, possiblly indicating more regularity in the brushtrokes themselves. This is consistent with findings in [**?**] reporting large wavelet coefficients at fine scales (hence more irregularity) for non Van Gogh's than for Van Gogh's paintings. Also, the results obtained here suggest that paintings $f386$ and $f605$ are closer to the Provence period cluster (Red), while $f572$ is closer to the Paris period cluster (Blue). It must be noted however that following these fractal property criteria, $f411$ from the Provence period would incorrectly be attributed to the Paris period.

4.4. Authenticity Challenge

4.4.1. Description

In this challenge, digitized copies of 4 paintings by Van Gogh, and 4 by contemporaries, are provided, and one painting is labelled unknown and

proposed for classification. The latter painting is a known contemporary copy of an original Van Gogh's painting. However, the original Van Gogh is not in the available data set, hence preventing us from performing comparisons as conducted in the Princeton experiment case. Experts state that the colors of the copies have remained truer to the original colors than those of the painting by the master. Essentially, their distinction between Van Gogh's and true Van Gogh's is based on a careful analysis of Van Gogh's brushstroke referred to as *vigourous* with non overlapping and netly defined strokes, as opposed to those of his contemporaries ever found too academic and regular or too messy and irregular (cf. `www.digitalpaintinganalysis.org/Challenges.htm`).

The challenge consists in devising numerical features that distinguish the two test sets and enable to associate the test painting with the one or the other group. The nine paintings are shown in Fig. 12.

4.4.2. Results

Fig. 13 proposes logscale diagrams, scaling functions and multifractal spectra for the Red Channel for an arbitrary choice of one painting each out of the reference classes, and for the painting whose label is to be determined.

A careful inspection of the multifractal spectra leads to suggest that Van Gogh's painting tends to be globally more regular. Systematic estimation of the h_m, c_1, c_2 parameters on the 7 channels of the 9 paintings and manual analysis and 2D projections as described in the dating challenge reveal that the Saturation and Red Channels are most discriminant between the two sets, and that the Non Van Gogh paintings are overall more irregular, with smaller values for h_m and c_1 (cf. Fig. 14). These 2D projections also indicate that the painting under investigation, $s506$, is further from the Non Van Gogh's paintings cluster and closer to the Van Gogh cluster. This incorrectly contradicts experts decision but may interestingly indicate that the copyist was more successful here in reproducing Van Gogh's brushstroke regularity.

5. Conclusions and Perspectives

This contribution illustrated the potential and possibilities of the wavelet leader multifractal formalism analysis applied to digitized paintings to assist art investigation.

At the technical level, it showed that the wavelet leader multifractal formalism must be used in complements of the classical wavelet coefficients to well assess the relevance of fractal properties as well as the range of scales

where they can be regarded as relevant. Also, multifractal analysis cannot be used blindly to pieces of images or paintings that consist of a collection of different textures or of mixtures of different objects and subjects. Instead, a careful selection of patches consisting of homogeneous textures must be achieved. This is where interventions of art experts could prove useful: They may peak specific patches that contain a particular interest with respect to the techniques used, the status of the colors,...

At the painting level, it is worth mentioning that the range of scales where fractal properties where found to hold are the same (from 0.5 mm to 5 mm) for the Princeton experiment and for the Van Gogh's painting (though scanned at different resolutions). This has been obtained independently by two different multifractal experts. Again, interpretation of why this range of scales should carry fractal properties in painting should significantly benefit from close discussions with art experts. Also, art experts could further contribute significantly to the kind of analysis proposed here by suggesting, for each painting, which patch should analyzed in priority given a specific interest or question.

This contribution showed, we believe, promising results: Multifractal analysis enables to measure features that fruitfully characterize painting textures. This first attempt can be further complemented by increasing the number and type of attributes estimated. Measures of anisotropy are currently being investigated.

Hopefully, such results may promote further and closer interactions between image processing researchers and art experts. Such exchanges could enable the constitution of data sets, where both technical issues (scanner resolution and techniques) and art expertise is well documented, the formation of real interdisciplinary teams where art experts would propose questions for which image processing could help to formulate answers.

6. Acknowledgements

The authors are gratefully acknowledge the leaders of the *Image Processing for Art Investigation* project, for having warmly welcomed us in this research program. R. Johnson, D. Rockmore and I. Daubechies are specifically acknowledged. The Van Gogh and Kröller-Müller Museums (The Netherlands) have permitted this work by making numerous paintings available in the framework of the *Image Processing for Art Investigation* project. The

princeton research team (notably S. Hughes and I. Daubechies) are acknowledged for giving us access to the Princeton experiment data. S. Hughes and E. Postma are also gratefully acknowledged for their kind help in Data handling. J. Coddington (Chief Conservator at the MoMA) and E. Hendricks (Chief Conservator at the Van Gogh museum) significantly helped us with valuable discussions on space scales, notably. They are gratefully acknowledged.

This work has been partially supported by the Del Duca Foundation, Institut de France, Young Research Team Award 2007.

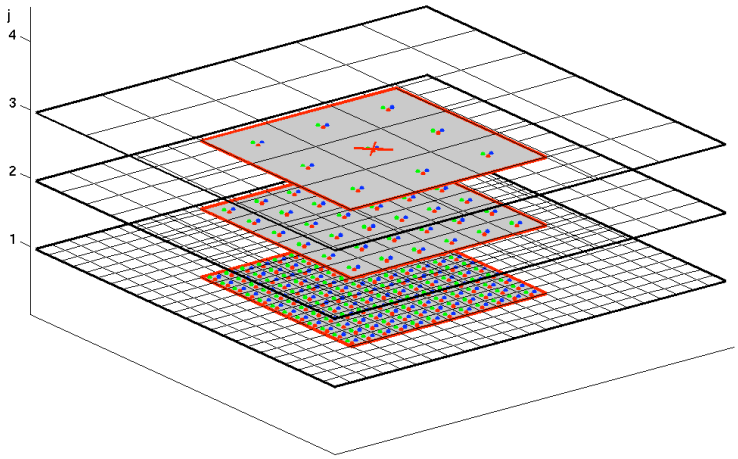

Figure 1: **Wavelet leaders:** The wavelet leader $L_X(j, k_1, k_2)$, located at scale 2^j and position $2^j x_1, 2^j x_2$, is obtained as the largest of all wavelet coefficients located in a *narrow* spatial neighborhood and at any finer scale $2^{j'} \leq 2^j$.

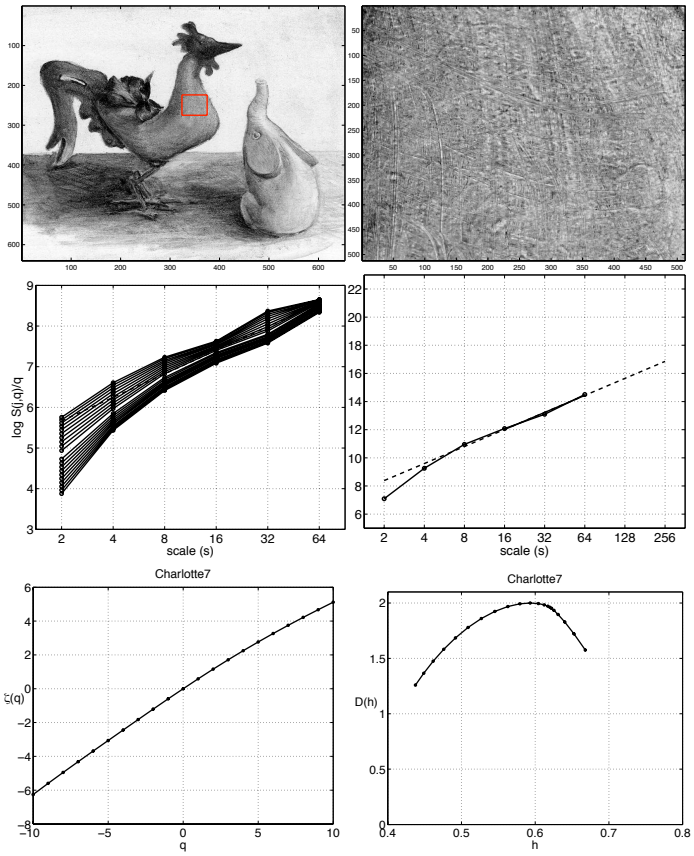

Figure 2: **Multifractal Analysis and Analysis - Painting 7 of the Princeton Experiment.** From top to bottom: Painting, Selected Patch, Logscale Diagrams $(\log_2 S(j,q,\gamma)/q$ vs. $\log_2 2^j = j$ for numerous qs, Linear Regression for $q = 2$, Scaling Function $\zeta(q)$, Multifractal Spectrum $D(h)$.

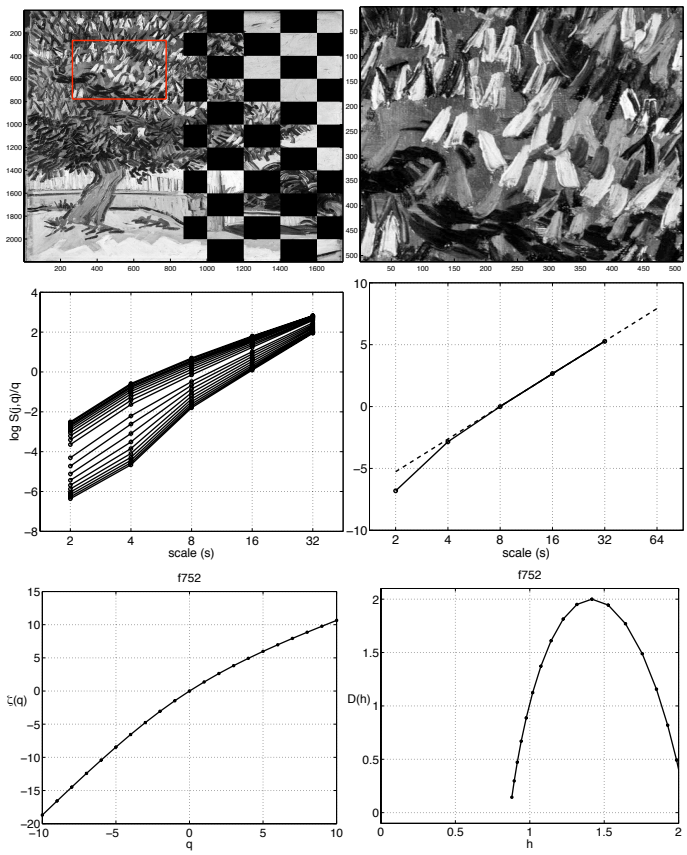

Figure 3: **Multifractal Analysis and Analysis -Van Gogh's f752 Painting.** From top to bottom: Painting, Selected Patch, Logscale Diagrams ($\log_2 S(j,q,\gamma)/q$ vs. $\log_2 2^j = j$ for numerous qs, Linear Regression for $q = 2$, Scaling Function $\zeta(q)$, Multifractal Spectrum $D(h)$.

Figure 4: **The Princeton Experiment:** The 7 originals, numbered hereafter 1 to 7, from left to right and top to bottom.

Pair	Ground	Paint	Brushes	Pixel
1	CP Canvas	Oils	S & H	6272×6528
2	CP Canvas	Acrylics	S & H	6272×6528
3	Smooth CP Board	Oils	S & H	6272×6528
4	Bare Linen Canvas	Oils	S	3200×6144
5	Chalk & Glue	Oils	S	3328×4608
6	CP Canvas	Acrylics	S	3456×5504
7	Smooth CP Board	Oils	S	6400×6528

Table 1: The Princeton Experiment. Soft brushes were sable or synthetic; hard brushes were flat hog hair.

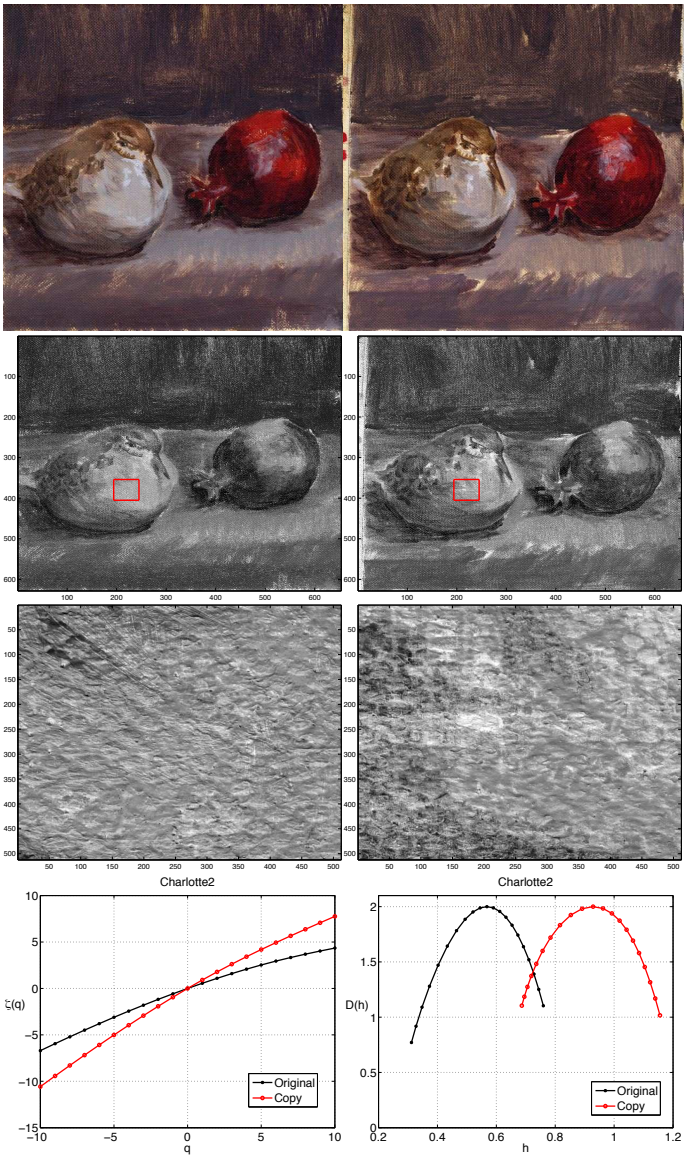

Figure 5: **Multifractal Analysis.** Three first lines: original (left) and copy (right). Last line: estimated multifractal attributes: original (black) and copy (red).

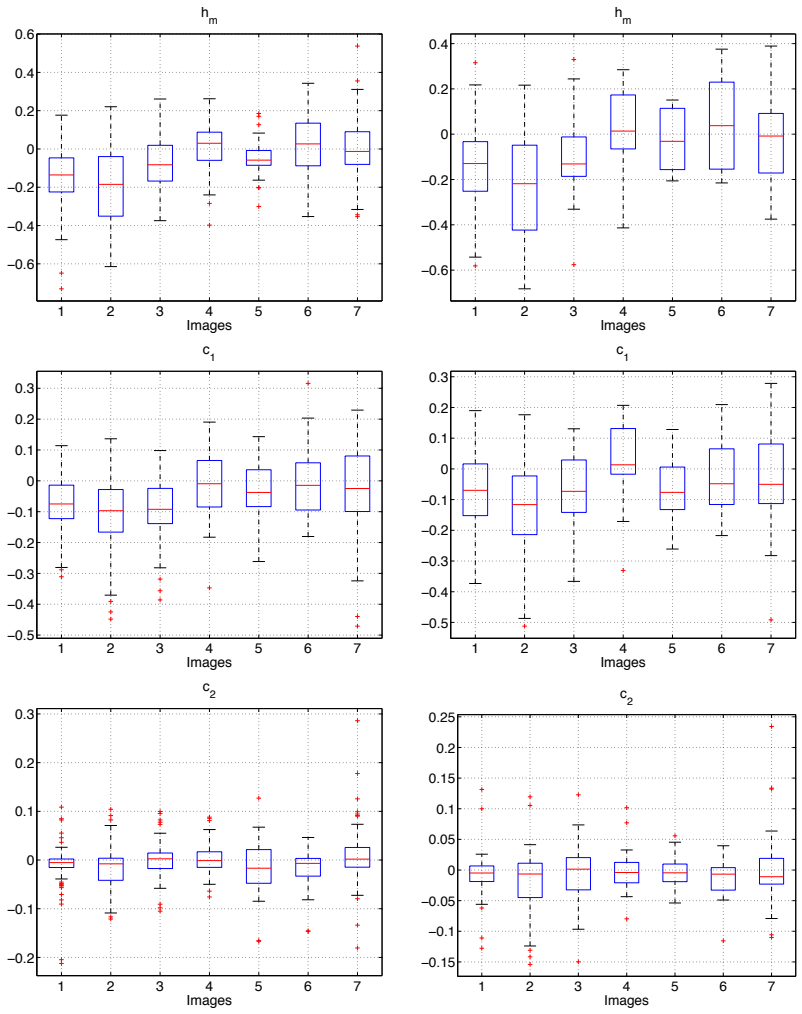

Figure 6: **Differences in multifractal parameters for the 7 paintings.** Top: h middle: c_1, bottom: c_2 ; Left: All 7 channels, right: Luminance L channel only.

1	h_m	c_1	c_2	2	h_m	c_1	c_2
All-Chan.	0.00	0.00	0.15	All-Chan.	0.00	0.00	0.00
Lum.	0.00	0.03	0.62	Lum.	0.24	0.00	0.41
All-Chan	0.00	0.00	0.01	All-Chan.	0.00	0.00	0.00
Lum.	0.00	0.01	0.20	Lum.	0.00	0.00	0.10
All-Chan	0.00	0.00	0.02	All-Chan.	0.00	0.00	0.00
Lum.	0.03	0.14	0.28	Lum.	0.00	0.02	0.03
All-Chan	−0.14	−0.07	−0.01	All-Chan.	−0.20	−0.11	−0.02
Lum.	−0.15	−0.06	0.01	Lum.	−0.23	−0.12	0.02
3	h_m	c_1	c_2	4	h_m	c_1	c_2
All-Chan.	0.00	0.00	0.73	All-Chan.	0.21	0.39	0.0
Lum.	0.00	0.03	1.00	Lum.	0.48	0.48	0.48
All-Chan	0.00	0.00	0.58	All-Chan.	0.44	0.47	0.06
Lum.	0.00	0.00	0.74	Lum.	0.31	0.40	0.81
All-Chan	0.01	0.03	0.53	All-Chan.	0.58	0.90	0.21
Lum.	0.08	0.21	0.54	Lum.	0.87	1.00	0.87
All-Chan	−0.07	−0.06	−0.00	All-Chan.	0.01	0.01	−0.01
Lum.	−0.10	−0.08	0.00	Lum.	0.02	0.01	0.01
5	h_m	c_1	c_2	6	h_m	c_1	c_2
All-Chan.	0.01	0.00	0.08	All-Chan.	0.60	0.60	0.04
Lum.	0.39	0.15	0.77	Lum.	1.00	0.60	0.31
All-Chan	0.02	0.00	0.02	All-Chan.	0.32	0.07	0.01
Lum.	0.38	0.06	0.62	Lum.	0.33	0.39	0.11
All-Chan	0.38	0.24	0.49	All-Chan.	0.39	0.79	0.37
Lum.	0.72	0.87	0.98	Lum.	0.94	0.94	0.61
All-Chan	−0.05	−0.05	−0.02	All-Chan.	0.03	−0.02	0.15
Lum.	−0.01	−0.02	0.00	Lum.	0.02	−0.01	0.01
7	h_m	c_1	c_2				
All-Chan.	0.00	0.01	0.54				
Lum.	0.87	0.24	0.24				
All-Chan	0.01	0.00	0.98				
Lum.	0.50	0.31	0.57				
All-Chan	0.29	0.13	0.26				
Lum.	0.75	0.77	0.90				
All-Chan	−0.03	−0.05	0.00				
Lum.	−0.02	−0.03	−0.00				

Table 2: **P-values.** For each 7 sub-tables (corresponding to the 7 images), the p-values correspond to the pairWise SignTest (Top), PairWise RankTest (MiddleTop), NonPairWise Wilcoxon RankSum (Middle-bottom:). The Bottom pair of lines shows the mean value of the difference between Original and Copy. In each pair of lines, the top line corresponds to the test applied to all 7 channels, while the bottom shows results for the test

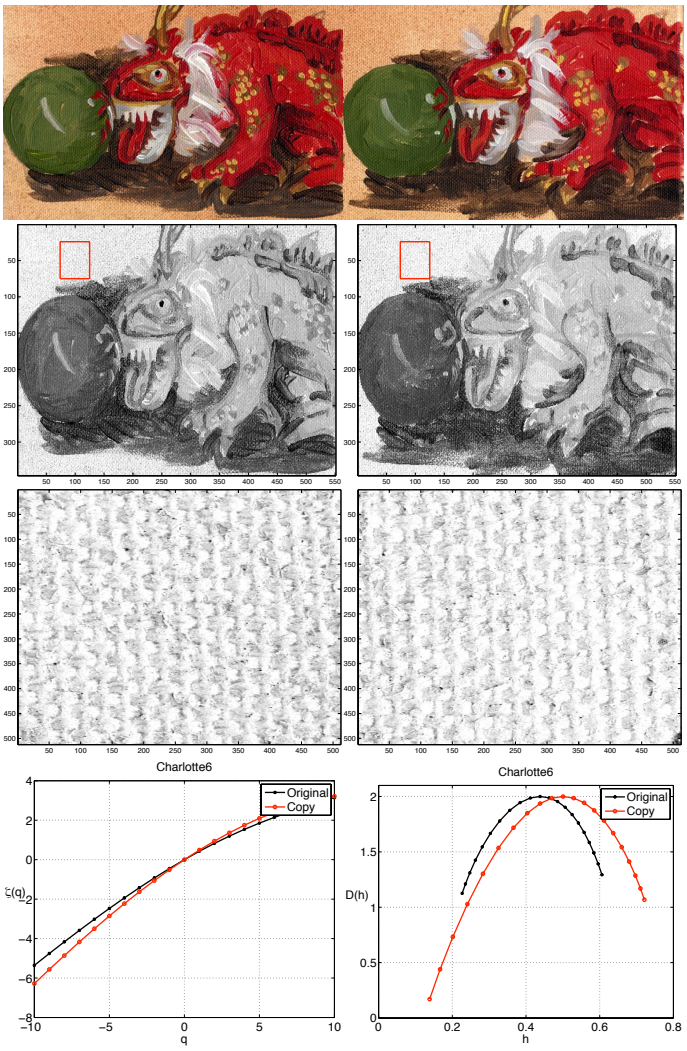

Figure 7: **Multifractal Analysis.** Three first lines: original (left) and copy (right). Last line: estimated multifractal attributes: original (black) and copy (red).

Pair	Ground	Paint	Brushes	Discr.
1	CP Canvas	Oils	S & H	PW/NPW
2	CP Canvas	Acrylics	S & H	PW/NPW
3	Smooth CP Board	Oils	S & H	PW/NPW
4	Bare Linen Canvas	Oils	S	·
5	Chalk & Glue	Oils	S	PW
6	CP Canvas	Acrylics	S	·
7	Smooth CP Board	Oils	S	PW

Table 3: **Discriminating Original from Copy.** Copies have textures which are significantly globally more regular than those of originals for Paintings 1 to 3. This is well detected both using pairwise (PW) and non pairwise (NPW) tests. It is also the case for Paintings 5 and 7, but only for PairWise (PW) tests, i.e., only when comparing patches with same locations on original and copy.

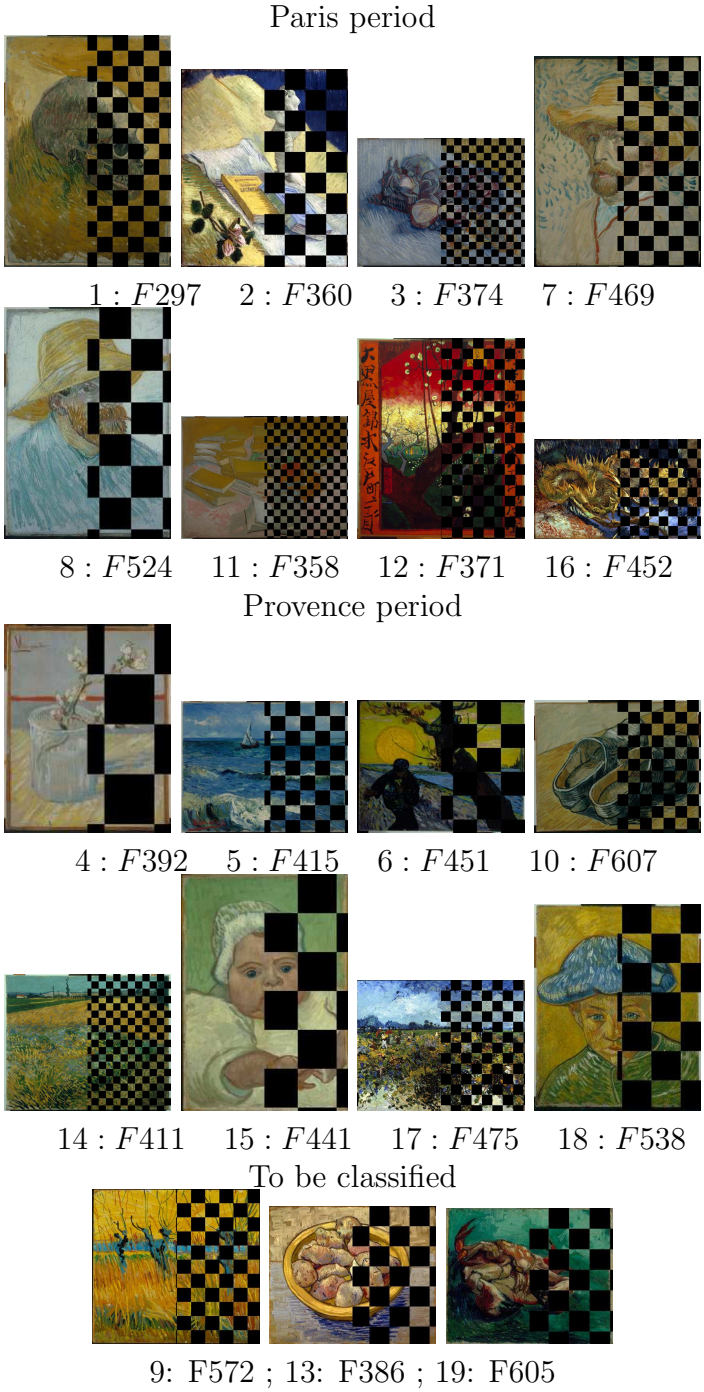

Figure 8: **Dating challenge: Provence vs. Paris periods.** 8 paintings from the Paris period (top), 8 paintings from the Provence period (middle), 3 paintings to be classified.

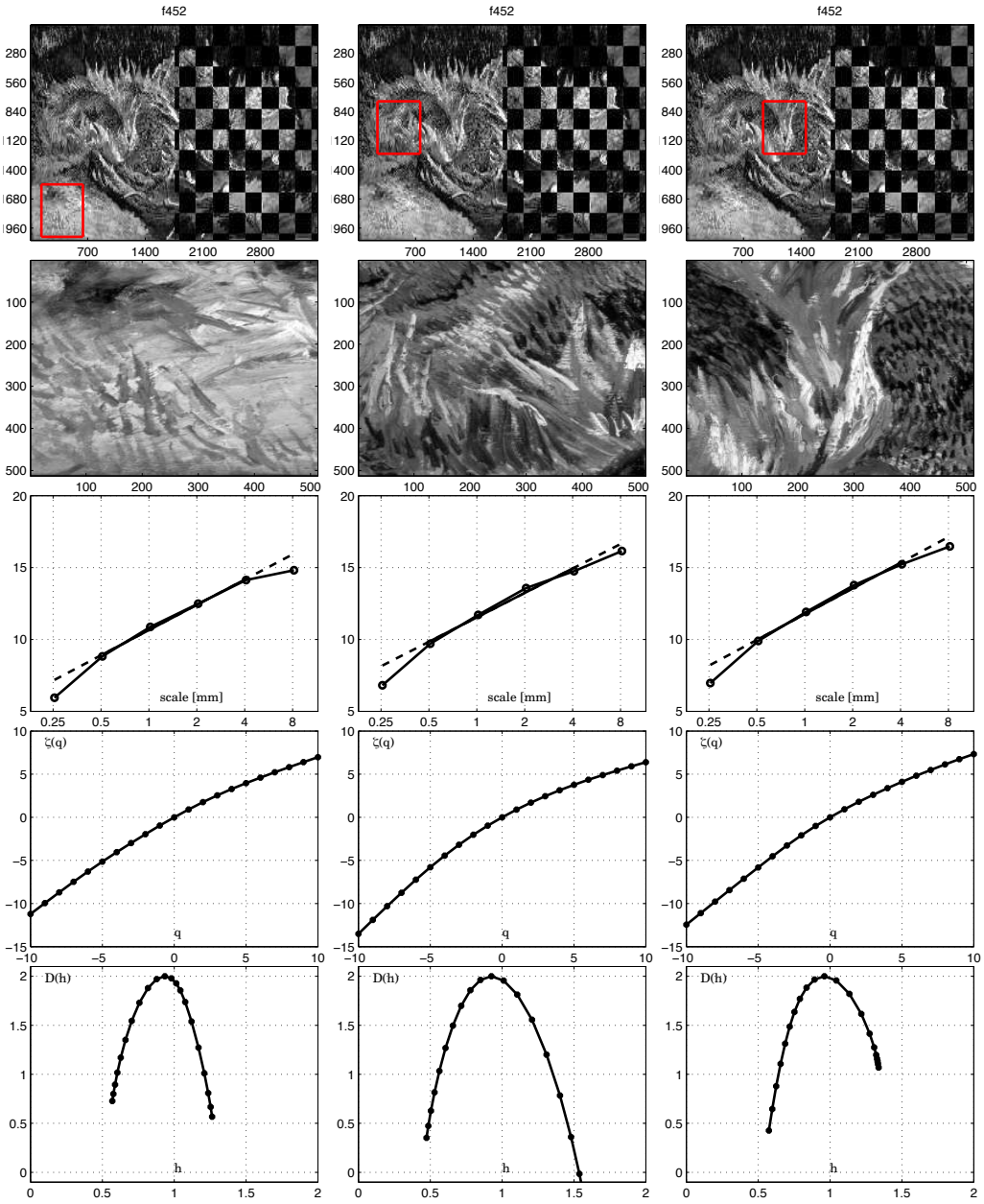

Figure 9: **Multiple patches from one single painting.** The multifractal spectra computed on 3 different patches extracted from the Red Channel Van Gogh's Painting from the Paris period f452 suggests that estimates from the 3 patches of visually different texture are consistent. The precise values for the multifractal attribute triple (c_1, c_2, h_m) are (from left to right): $(0.93, -0.051, 0.050)$, $(0.93, -0.081, -0.051)$, $(0.96, -0.076, -0.007)$.

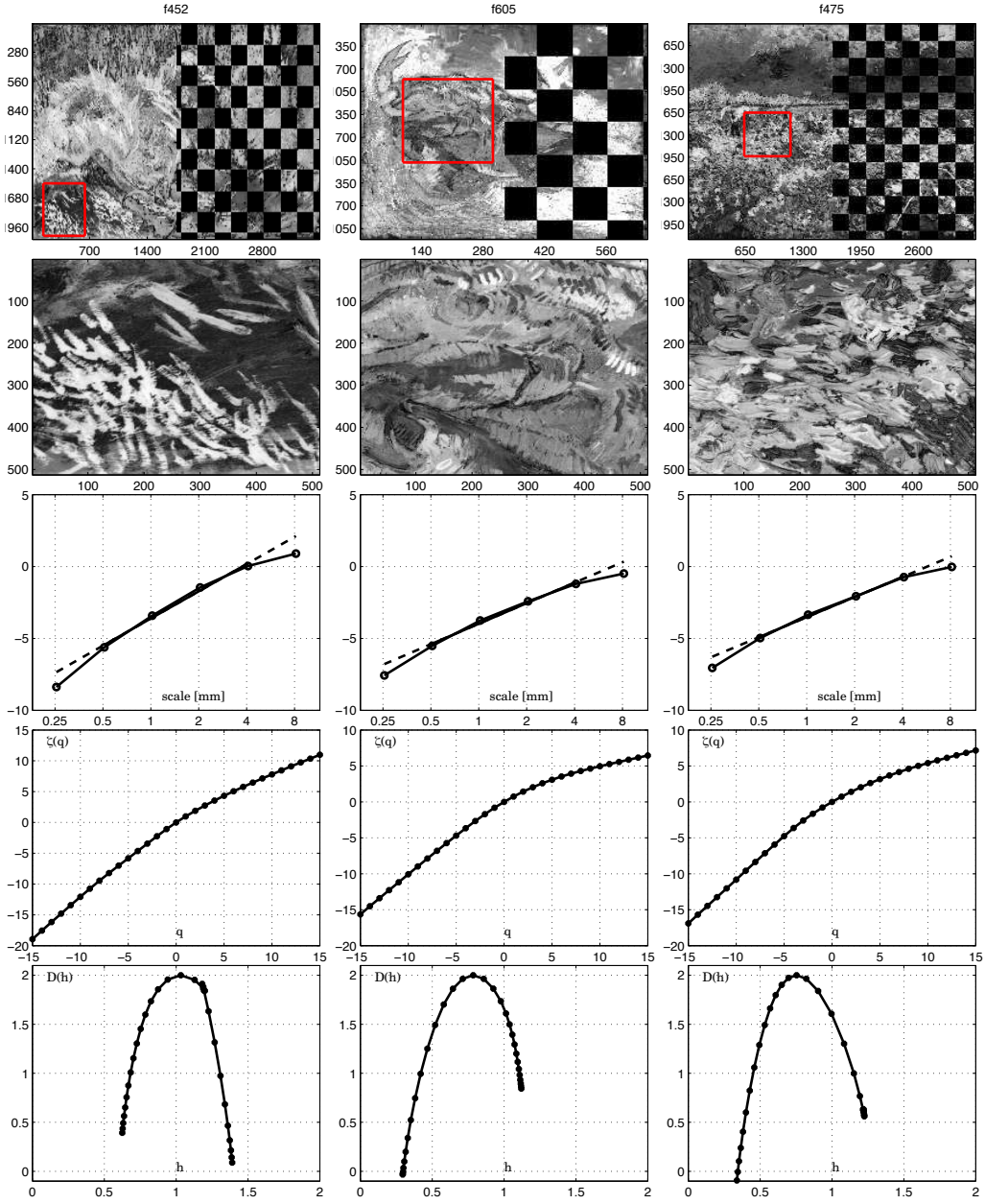

Figure 10: **Dating challenge: Paris vs. Provence periods.** Multifractal spectrum computed on patches extracted from the Saturation Channel of Van Gogh's Paintings from the Paris period (F452, left), from the Provence period (F475, right), to be classified (F605, middle) from its multifractal properties.

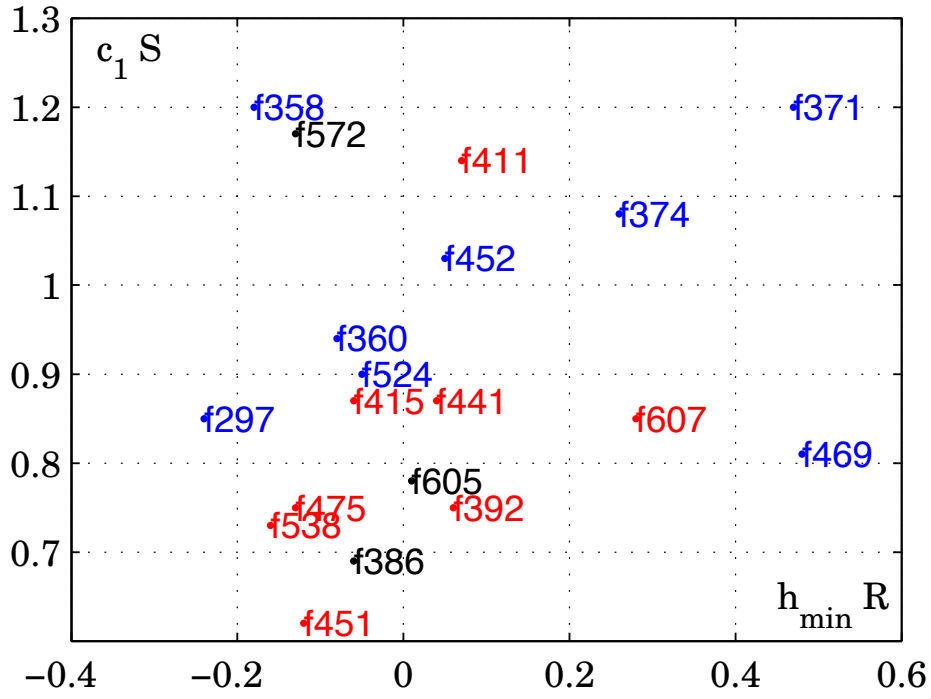

Figure 11: **Dating challenge: Paris vs. Provence periods.** Plots of h_m computed from the Red Channel vs. c_1 from the Saturation Channel suggests that paintings `f386` `f605` are closer to the Provence period cluster (Red), while `f572` is closer to the Paris period cluster (Blue).

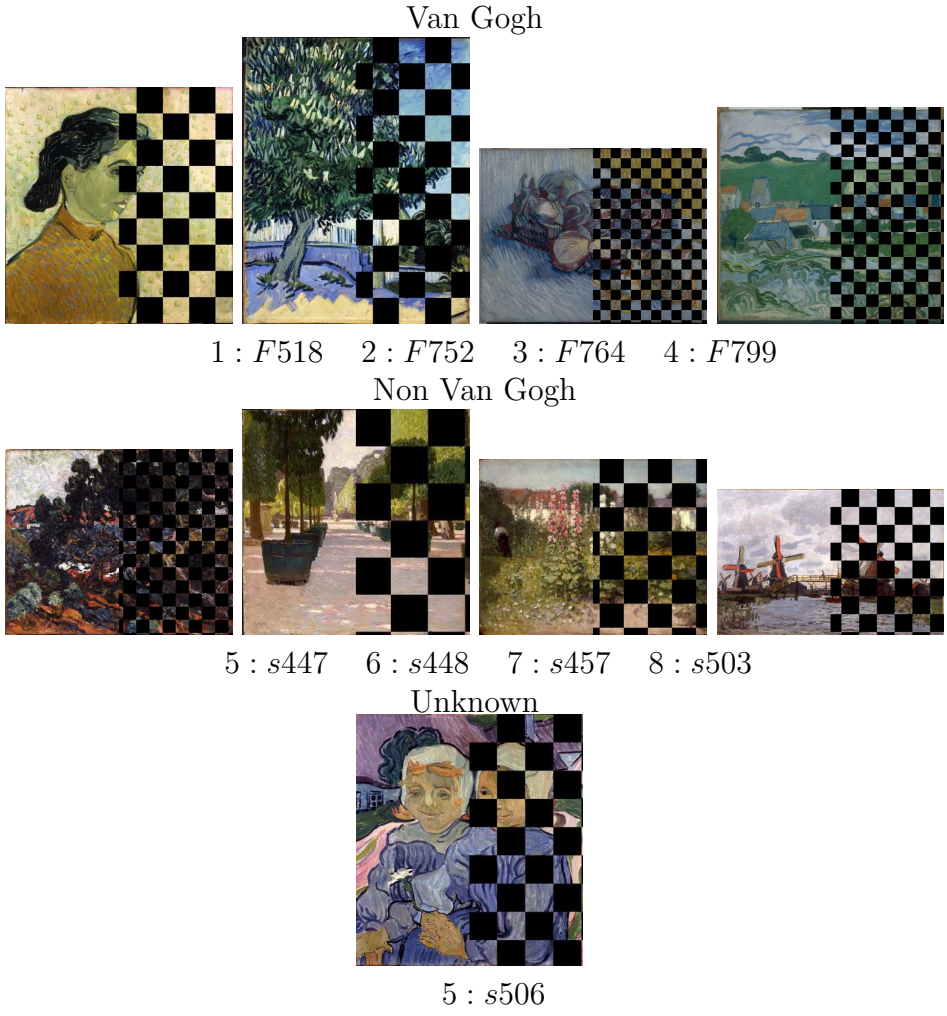

Figure 12: **Authenticity challenge: Van Gogh's vs. non Van Gogh's Paintings.** 4 paintings from Van Gogh (top), 4 paintings not from Van Gogh (middle), and the painting to be classified.

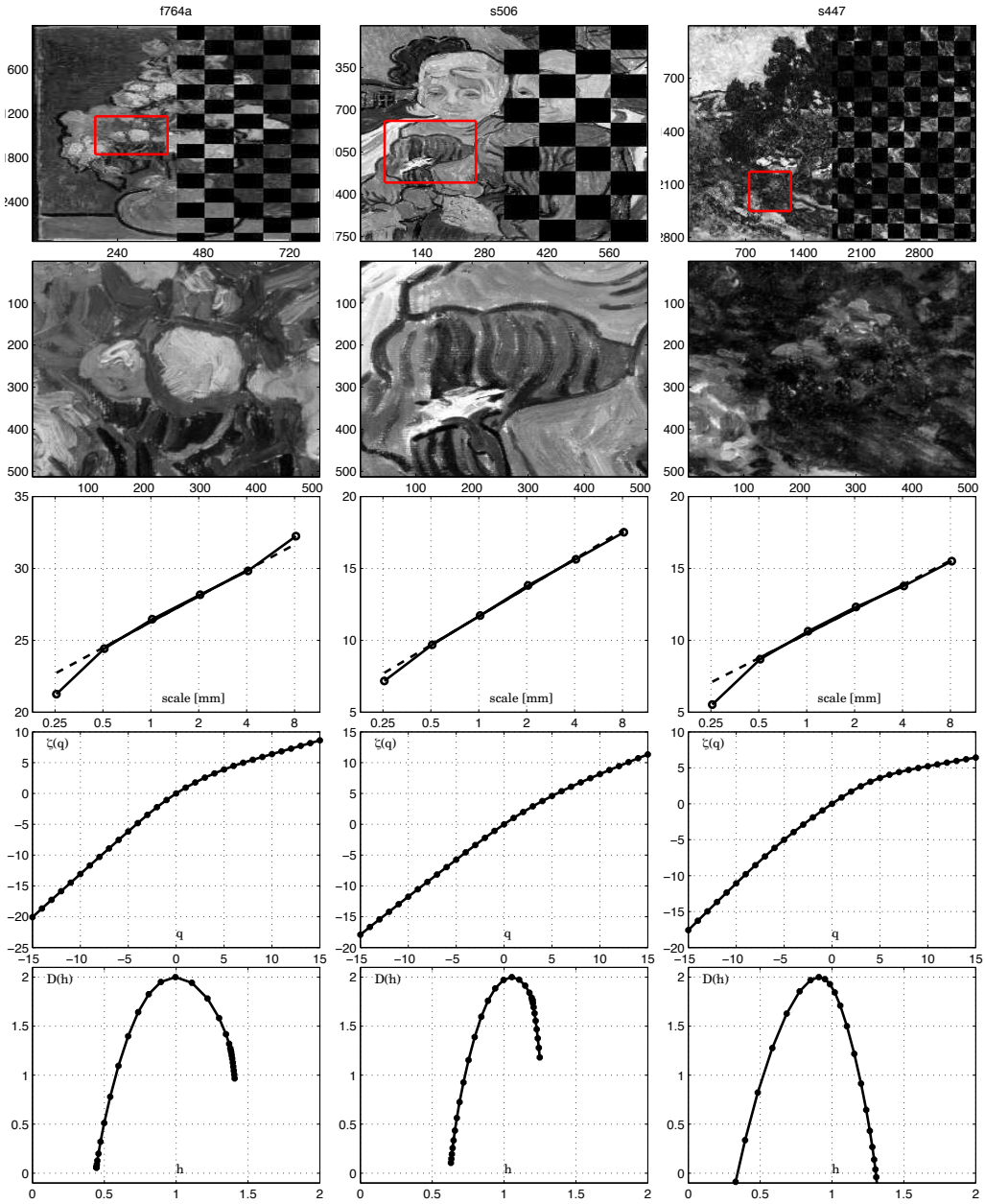

Figure 13: **Authenticity challenge: Van Gogh's vs. non Van Gogh's Paintings.** Multifractal spectrum computed on patches extracted from the Red Channel of Van Gogh's (left) and non Van Gogh's (right) Paintings compared to the painting under test (middle).

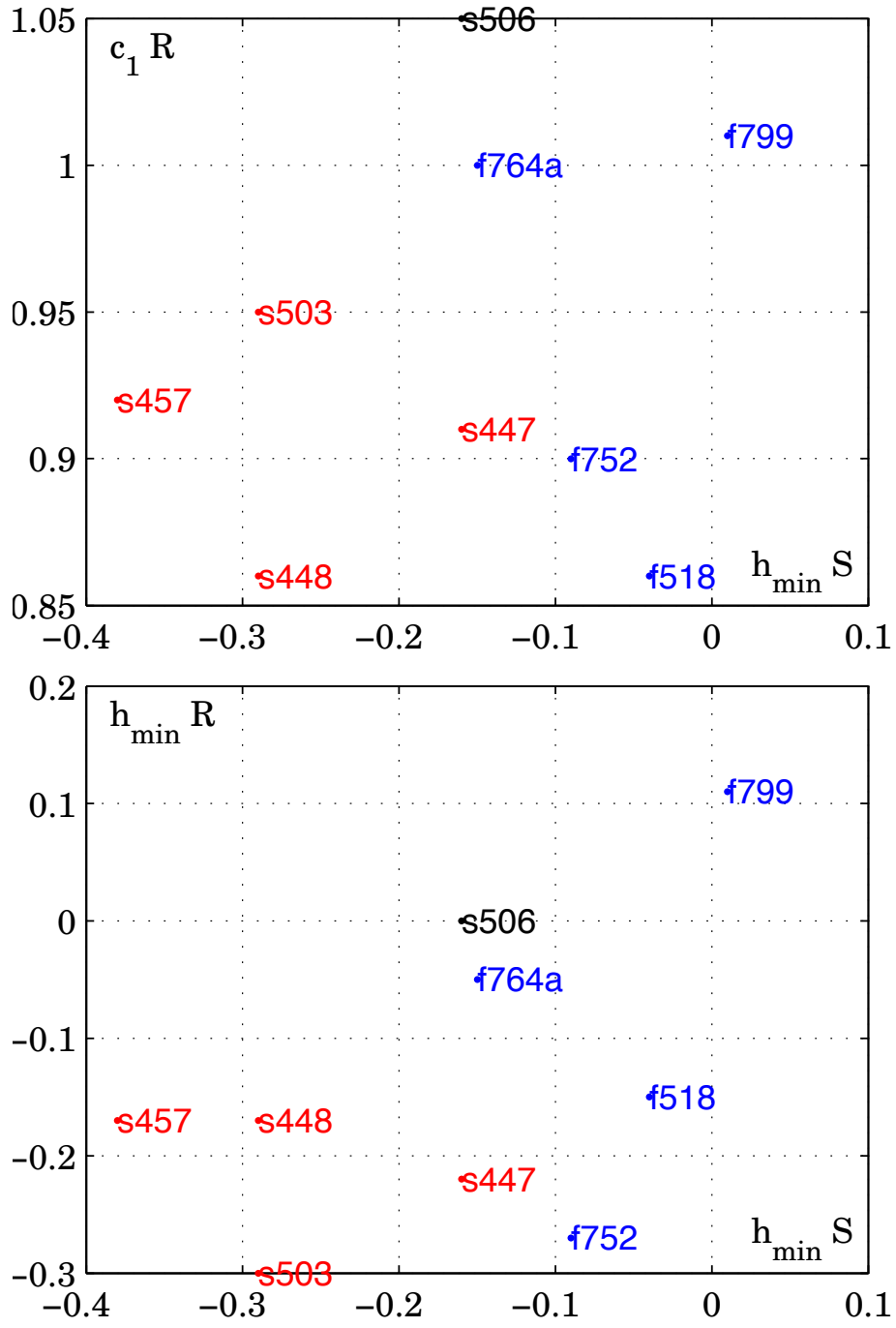

Figure 14: **Authenticity challenge: Van Gogh's vs. non Van Gogh's Paintings.** Plots of h_m computed from the Saturation Channel versus c_1 (left) and h_m (right) from the Red Channel suggest that painting `s506` is closer to the Van Gogh cluster (Blue) than to the Non Van Gogh cluster (Red).